Published in final edited form as:
Biomaterials. 2011 November ; 32(31): 7932–7940. doi:10.1016/j.biomaterials.2011.07.018.

Influence of Chondroitin Sulfate and Hyaluronic Acid on Structure, Mechanical Properties, and Glioma Invasion of Collagen I Gels

Ya-li Yang[*], **Charles Sun**[**], **Matthew E. Wilhelm**, **Laura J. Fox**[***], **Jieling Zhu**, and **Laura J. Kaufman**
Department of Chemistry, Columbia University, New York, NY 10027

Abstract

To mimic the extracellular matrix surrounding high grade gliomas, composite matrices composed of either acid-solubilized (AS) or pepsin-treated (PT) collagen and the glycosaminoglycans chondroitin sulfate (CS) and hyaluronic acid (HA) are prepared and characterized. The structure and mechanical properties of collagen/CS and collagen/HA gels are studied via confocal reflectance microscopy (CRM) and rheology. CRM reveals that CS induces fibril bundling and increased mesh size in AS collagen but not PT collagen networks. The presence of CS also induces more substantial changes in the storage and loss moduli of AS gels than of PT gels, in accordance with expectation based on network structural parameters. The presence of HA significantly reduces mesh size in AS collagen but has a smaller effect on PT collagen networks. However, both AS and PT collagen network viscoelasticity is strongly affected by the presence of HA. The effects of CS and HA on glioma invasion is then studied in collagen/GAG matrices with network structure both similar to (PT collagen-based gels) and disparate from (AS collagen-based gels) those of the corresponding pure collagen matrices. It is shown that CS inhibits and HA has no significant effect on glioma invasion in 1.0 mg/ml collagen matrices over 3 days. The inhibitory effect of CS on glioma invasion is more apparent in AS than in PT collagen gels, suggesting invasive behavior in these environments is affected by both biochemical and network morphological changes induced by GAGs. This study is among the few efforts to differentiate structural, mechanical and biochemical effects of changes to matrix composition on cell motility in 3D.

1. Introduction

Extracellular matrix (ECM) is the complex environment composed of collagens, glycoproteins, glycosaminoglycans (GAGs) and proteoglycans (PGs) that surrounds and supports cells [1]. Type I collagen is the most common structural protein in mammalian tissue and has been widely used as a three dimensional (3D) ECM approximation in which to study cell behavior. Aside from the fact that collagen I environments are broadly physiologically relevant due to their dimensionality and the fact that they are composed of the most prevalent mammalian ECM component, collagen I environments also provide several other benefits for *in vitro* cell studies. First, collagen I forms fibrils that are easily visualizable with a variety of microscopies, such that when cells are embedded in these matrices, the cells, collagen fibrils, and their reciprocal interactions can be visualized

Correspondence to: Laura J. Kaufman.
[*]current address: Department of Mechanical Engineering, University of California – Santa Barbara, Santa Barbara, CA 93106
[**]current address: Department of Biomedical Engineering, Boston University, Boston, MA 02215
[***]current address: Department of Chemistry, University of Minnesota, Minneapolis, MN 55455

simultaneously using multimodal microscopy [2–4]. Additionally, collagen I gels formed *in vitro* have tunable structure and mechanical properties controlled by gelation conditions including pH, temperature, and ionic strength [5–8]. Such tunability allows for construction of environments in which the independent effects of mechanical properties and network structure on cell behavior in 3D environments can be assessed [9–13].

While collagen I gels are generally used as single component environments for *in vitro* studies of cell behavior, multi-component gels may more closely approximate the extracellular environment present in a particular tissue of interest. For example, while the migration and invasion of cells derived from high grade gliomas have been studied in collagen I environments [2, 14–21], such environments are not especially good mimics of the brain tissue that gliomas invade *in vivo*. Unlike most tissue, brain does not contain large amounts of collagen I, instead being composed chiefly of neuronal and glial cells. However ECM does exist in the brain, both in the form of structural proteins and supporting GAGs and PGs, and some of the locations in which ECM is most prevalent in brain are also locations where high grade gliomas preferentially invade [22]. Hyaluronan (HA), a molecule composed of repeating units of glucuronic acid and N-acetylglucosamine, is the most abundant GAG in brain tissue [23]. The molecule has extraordinary water retaining capacity and interacts with a variety of cell-surface receptors such as CD44 to regulate cell behavior and potentially promote glioma malignancy [23–25]. Another prominent GAG in brain tissue is chondroitin sulfate (CS), a sulfated molecule containing N-galactosamine and D-glucuronate units. In brain tissue, CS exists predominantly as chondroitin sulfate proteoglycans (CSPGs), known as lecticans, which are overexpressed by gliomas and have been shown to have a motogenic effect on glioma cells [26, 27].

In order to move towards 3D environments that mimic key aspects of the structural, functional, and biochemical aspects of brain tissue while retaining the benefits of collagen I environments, we introduce CS or HA over a range of concentrations into collagen solutions during fibrillogenesis to make collagen/GAG composites. Such composites have been studied previously, though reports on how CS and HA alter gel mechanical properties and network structure are not in full agreement [28–38]. Because a subset of the reported discrepancies may be related to differences in collagen source, extraction technique, and preparation conditions, we investigate the effects of CS and HA on collagen gels made from both pepsin-treated (PT) and acid-solubilized (AS) collagen. PT collagen lacks the telopeptides found in native collagen and is commonly used in bioengineering applications due to its non-antigenicity. AS collagen retains native telopeptides and interfibrillar cross-links and is more commonly used in biophysical studies. Differences between networks composed of AS and PT collagen have begun to attract attention [39, 40], but potential differences between GAG/AS collagen interactions and GAG/PT collagen interactions have not been considered previously. We target a range of CS and HA concentrations such that the GAG:collagen ratio spans from less than one, consistent with the ratio in vasculature and other tissues, to greater than ten, to approach the biochemical composition of ECM surrounding gliomas and in normal brain parenchyma. Optical microscopy is used to investigate potential changes to collagen fibril structure and gel network structure that may occur in the presence of the secondary ECM components, and oscillatory rheology is used to monitor potential changes in gel viscoelasticity induced by the CS or HA. We investigate whether correlations between gelation kinetics, gel network structure, and gel storage modulus found in pure collagen gels are also present in the GAG/collagen composites. Glioma spheroid invasion in GAG/collagen gels at high GAG concentrations is monitored. Performing these studies in both AS and PT collagen helps isolate the biochemical effects of CS and HA on glioma invasion.

2. Materials and Methods

2.1 Materials

Acid-solubilized (AS) rat tail collagen I is obtained from BD Biosciences (San Jose, CA) and pepsin-treated (PT) bovine hide collagen I is obtained from Advanced BioMatrix (San Diego, CA). Hyaluronic acid sodium salt from *streptococcus equi*, chondroitin sulfate A sodium salt from bovine trachea, 10× Dulbecco's Modified Eagle Media (DMEM), 7.5% v/v sodium bicarbonate, and 1 N sodium hydroxide are obtained from Sigma Aldrich (St. Louis, MO). 1 M Gibco HEPES buffer is obtained from Invitrogen (Carlsbad, CA). C6 rat glioma cells are obtained from the American Type Culture Collection (Manassas, VA). The cell culture reagents, 1× DMEM (high glucose), heat-inactivated fetal bovine serum (FBS), 100× antibiotic-antimycotic solution, and trypsin-EDTA, are obtained from Invitrogen.

2.2 Preparation of 3D collagen, collagen/HA, and collagen/CS gels

Pure collagen, collagen/HA, and collagen/CS gels are prepared at 4°C. HA and CS are dissolved in water to prepare stock solutions of 10 mg/ml, 20 mg/ml, or 100 mg/ml (CS only). Appropriate volumes of collagen and HA stock solution or CS stock solution, depending on the final concentrations desired, are mixed with appropriate volumes of DMEM, sodium bicarbonate, HEPES buffer, deionized water, and sodium hydroxide to yield a pH of 7.4 and final percent volume concentrations of 10, 2.5, and 2.5% DMEM, sodium bicarbonate, and HEPES, respectively. Such preparation conditions are used since they are supportive of cell culture. Solutions are well mixed and are placed in an incubator at 37°C to gel or are held at 4°C (for no more than 5 minutes after gel neutralization) before rheology, where they are gelled *in situ*. In 1.0 mg/ml collagen gels, final CS concentration ranges from 0.05 – 20 mg/ml, while final HA concentration ranges from 0.5 – 12.5 mg/ml, the highest HA concentration that could be achieved without leading to inhomogeneity in the gel.

2.3 Preparation of glioma spheroids

Cells are cultured at 37°C with 5% carbon dioxide and are subcultured when 70–80% confluent. Multicellular tumor spheroids are formed using the hanging drop procedure starting with cells diluted to $2.5 – 5.0 \times 10^4$ cells/mL. A 100 mm petri dish is filled with 10 mL of culture medium consisting of 1× DMEM (high glucose) containing 10% (v/v) FBS and a 1% (v/v) 100× antibiotic/antimyotic solution. Drops of 20 μL of the cell culture are placed on the lid of the Petri dish. The lid is inverted and incubated for 5–10 days. The drops are held in place by surface tension and the cells accumulate at the bottom of the droplet to form spheroids. The spheroids are then pipetted into collagen, collagen/HA, or collagen/CS solutions prepared as described above, after which they are placed in an incubator at 37°C for gelation and maintenance of cell health. 50 μl of cell media is placed atop the spheroid-containing gels after each round of imaging (at 2, 24, 48, and 72 hours after implantation).

2.4 Rheology

Rheological experiments are conducted on an AR-2000 rheometer with built in temperature and gap calibration. A 1° acrylic cone geometry with a solvent trap is used. Time sweep experiments are conducted in oscillatory mode at a fixed frequency of 1 Hz. The collagen and collagen/GAG solutions are applied to the measuring stage at 4°C. The geometry is lowered, the solvent trap is added, and measurements begin when the temperature reaches 37°C. Storage modulus (G') and loss modulus (G") are measured as the gel forms until plateaus are reached. For some PT collagen gels, to assure breakage of the developing gels during rheological measurements does not occur, systems are gelled on the rheometer for 45 minutes before oscillatory rheology measurements are performed. For all other gels,

measuring moduli with either of these procedures leads to identical plateau storage and loss moduli (unpublished data). All tests are repeated three or four times.

2.5 Microscopy and Image Analysis

Collagen or collagen/GAG solutions to be imaged are loaded just after neutralization at 4°C into cylindrical sample cells with a cover slip thickness bottom. The solutions are brought to 37°C and held there at least 1.25 hours for AS collagen-based gels and at least 2 hours for PT collagen-based gels, to assure gelation is complete. CRM images are recorded with an inverted confocal laser scanning microscope (Olympus Fluoview 300) with a 60× NA = 1.2 water objective. An argon ion laser at 488 nm is the excitation source, and the reflected light is detected on a photomultiplier tube detector (PMT). Three images per gel are collected and three gels at each concentration are investigated.

Mesh size is quantified from CRM images. In some images, a CRM artifact leading to a bright spot at the center of images, caused by a reflection in the optical path, is replaced with a copy of the upper left corner of the image in order to have representative fibers throughout the entirety of the image. The images are then thresholded in order to remove noise while retaining fiber pixels. The threshold is determined by comparing the intensities of the brightest background pixels to the dimmest fiber pixels through visual inspection. Pixels with intensity greater than threshold are labeled “on,” the distance between on pixels in each row and column is calculated, and the histogram of these distances is plotted. This distribution is fit to an exponential decay with the characteristic length scale determined by this fit defined as the mesh size. Mesh size determined in this manner has previously been shown to correlate well with another measure of mesh size [8].

Transmitted light microscopy is used to image spheroids on the Olympus Fluoview 300 in scanning mode using an Argon ion laser at 488 nm for excitation and a PMT for detection. Six spheroids in each type of collagen gel are imaged 2, 24, 48, and 72 hours after implantation, and the collagen around the spheroid is imaged via CRM 2 hours after spheroid implantation. From the spheroid images, invasive distance, defined as the average distance between the periphery of the central, dense portion of the spheroid and a circle that circumscribes ~90% of the invasive cells, is determined for each image.

3. Results

3.1 Influence of CS and HA on Network Structure of Collagen Gels

CS or HA is added to both acid-solubilized (AS) and pepsin-treated (PT) collagen solutions to achieve final collagen content of 1.0 mg/ml and CS concentration ranging from 0 to 20 mg/ml or HA concentration ranging from 0 to 12.5 mg/ml. For collagen/HA solutions, homogeneous gels can not be reliably prepared at HA concentrations higher than 12.5 mg/ml owing to the high viscosity of the HA. Solutions are then gelled at 37°C.

Figure 1 shows representative CRM images of 1.0 mg/ml AS and PT collagen gels as well as 1.0 mg/ml AS and PT collagen gels with 10 mg/ml CS or HA. Collagen fibril morphology in pure 1.0 mg/ml AS collagen gels is quite different from that in pure PT collagen gels. The PT gels are more homogeneous than are those of AS collagen, and the fibrils formed from PT collagen appear somewhat thicker, straighter, and less entangled than those of AS collagen (Fig. 1a,d). The average mesh size in the two types of gels is nearly identical (Fig. 2), as would be expected of gels of the same concentration so long as the same proportion of collagen is organized into visualized fibrils and those fibrils are of similar width in both preparations.

The network structure of AS collagen/CS gels as revealed by CRM imaging changes with CS concentration. The presence of CS at concentrations of as little as 0.5 mg/ml leads to imaged fibrils that appear straighter and brighter than those visualized in the pure collagen gels (data not shown). At CS concentrations of ≥ 5.0 mg/ml, imaged fibrillar structures appear significantly brighter and thicker than at lower CS concentrations and are present in some cases as bundled multi-fibrillar structures that we term fibers. Such fibers are similar to those present in pure AS gels formed at temperatures lower than 37°C [8]. Assuming no change in proportion of collagen incorporated into fibrillar structures or average fibril length as a function of CS concentration, increased fibril thickness will lead to increased mesh size in the system. Such increased mesh size can be seen in Fig. 1b relative to Fig. 1a and is described quantitatively via mesh size analysis indicating an increase in mesh size from 5.1 – 12.0 μm for 1.0 mg/ml AS collagen with CS concentration from 0 – 20 mg/ml (Fig. 2).

Unlike in AS collagen, addition of CS to PT collagen causes little obvious change in fibril or network structure. Subtle increased brightness as a function of CS is apparent, suggesting a small increase in fibril thickness. For systems with a given amount of collagen present in fibrils, a small increase in average fibril thickness at fixed average fibril length will result in a small increase in mesh size, as is confirmed with mesh size analysis shown in Fig. 2.

Addition of HA to AS and PT collagen gels has markedly different effects on network structure than does addition of CS. For AS collagen, addition of HA results in an apparent increase in the number of fibrillar structures (Fig. 1c). The structures appear not only more numerous but also thinner and shorter than in the pure AS gels, and this is reflected quantitatively in the decreased mesh size as a function of HA concentration (Fig. 2). In PT collagen, addition of HA has subtler effects, though a small increase in fibril number and decreased mesh size is apparent (Fig. 1f, Fig. 2).

3.2 Influence of CS and HA on Viscoelasticity of Collagen Gels

The storage (G') and loss (G") moduli of a viscoelastic material represent the energy stored in and dissipated by the material, respectively. Figure 3a presents change in equilibrium storage modulus for AS and PT collagen gels as a function of CS and HA concentration. Because pure AS and PT collagen gels have somewhat different storage moduli at 1.0 mg/ml (~ 3 Pa for AS collagen and 6 Pa for PT collagen), normalized G' is presented to highlight change relative to pure collagen. As a function of CS concentration, AS/CS collagen G' values increase to a maximum at 5.0 mg/ml CS before decreasing to a minimum at the highest CS concentration employed, 20 mg/ml. For PT collagen gels, the changes as a function of CS concentration are similar to but of smaller magnitude than those seen for the AS gels. Just as the change in network structure of the gel with addition of CS is more apparent for AS collagen than PT collagen, so too is the change in storage modulus.

Conversely, even though AS collagen gel structure is more strongly affected by the presence of HA than is PT collagen gel structure, AS and PT collagen gels exhibit similar changes in equilibrium storage modulus with increasing amounts of HA (Fig. 3). Both AS and PT collagen gels with added HA exhibit G' values that increase substantially with HA concentration. In addition to potential changes in collagen gel storage modulus as a function of secondary ECM concentration, the loss modulus may change as well. For AS and PT collagen systems with CS, there is little change in the loss tangent ($\tan \delta = G''/G'$) as a function of CS concentration (Fig. 3b). This indicates that the viscoelastic behavior of the composite collagen/CS gels is similar to that of pure collagen gels. In contrast, the loss tangent increases markedly upon adding HA to both AS and PT collagen (Fig. 3b). This occurs even though the absolute value of G' increases substantially with added HA. The increase in the loss tangent is thus driven by a stark increase in loss modulus that occurs in these gels upon addition of HA. The increase in loss modulus is due primarily to viscous HA

dispersed between the collagen fibrils. Indeed, pure 10 mg/ml HA, for example, has G' of ~ 5 Pa and G" of ~ 10 Pa (data not shown). As such, it appears that the viscoelastic response of collagen/HA gels at the concentrations investigated is dominated by the HA viscoelasticity while that of collagen/CS gels is dominated by collagen viscoelasticity.

In addition to changes in the equilibrium mechanical properties of the collagen gels, the presence of secondary ECM components may induce changes in gelation kinetics. For AS collagen, no clear change in gelation kinetics is seen upon the addition of CS. For pure AS collagen and AS/CS composites, the gels attain their equilibrium modulus within several minutes of the beginning of the rheological experiments in all cases, and the resolution of our experiments is insufficient to detect potential increases of gelation speed as driven by the CS. In PT collagen, which gels substantially more slowly than AS collagen, the time required for the storage and loss moduli to plateau decreases with the addition of even very small amounts of CS (Fig. 4). In these gels, the lag time (the time over which G' is small and nearly constant), associated with nucleation, decreases with added CS. Additionally, the slope of the G' rise, which correlates with growth and interconnection of fibrils, increases with added CS. Thus, both the nucleation and growth phases of PT collagen gelation speed up upon addition of CS.

As for the addition of CS, the addition of HA does not noticeably affect the gelation speed of AS collagen, though this may again be related to the limited time resolution of the experiment. For PT collagen, in general, a decrease in gelation time as assessed by time to storage modulus plateau is seen; however, this is largely driven by an increase in initial G' of the system rather than a decrease in lag time or increase of the slope of the growth phase. This again highlights the more complex nature of the viscoelasticity of the collagen/HA composites compared to the collagen/CS composites.

3.3 Correlation Between Structure and Mechanical Properties in Collagen/CS Gels

Previously, we have shown that both fibril or fiber diameter and mesh size are important in setting collagen gel storage modulus [8]. As such, if CS or HA alters either the fibrillar diameter or mesh size of the matrix, these changes alone are expected to affect the mechanical properties of the gel. In addition, the CS and HA themselves may alter the mechanical properties of the composite independently of their effect on collagen gel fibril and network structure. For cells embedded in collagen/CS or collagen/HA matrices, the potential effects of such changes on cell behavior must be considered before any conclusions can be drawn regarding the biochemical effects of the CS or HA on cell behavior.

Because HA itself is highly viscous under the conditions studied here while pure CS remains a Newtonian solution with low viscosity even at the highest concentrations employed, we consider whether changes in collagen/CS, but not collagen/HA, gel mechanical properties and structure are consistent with those found previously for pure collagen. First, we note that although CS clearly increases the rate of PT collagen gelation even at very low CS concentrations, this does not alter the structure of the collagen gel in the manner that increased gelation speed does in pure collagen gels. In pure collagen gels, increased gelation speed occurs with either increased collagen concentration or higher gelation temperature up to ~ 37°C [5]. In both cases, fibril diameter decreases with increasing gelation speed [5, 41]. For the PT collagen/CS gels, however, no obvious change in fibril diameter is apparent. Moreover, in AS collagen, where we can not detect increased gelation speed as a function of CS due to limited time resolution, fibril bundling becomes apparent at high CS concentrations. For pure AS collagen, such bundling is only seen for low temperature gelation, where the gelation rate is significantly decreased from that at 37°C [5, 8]. For pure collagen gels, it is presumed that fast gelation correlates with thin fibrils because the growth portion of the nucleation and growth process of fibrillogenesis begins as soon as the

nucleation centers reach critical size rather than allowing for larger nucleation centers to develop. In the collagen/CS gels, however, there is evidence for both increased gelation speed and fibril bundling. Thus, we propose that the CS alters AS collagen fibrils in a manner that allows for bundling through a mechanism distinct from that which allows for bundling in pure AS collagen gels at low gelation temperature.

We now assess whether the changes in equilibrium structure seen as a function of CS in the AS collagen/CS gels correlate with changes in mechanical properties in the same manner that changes in structure correlate with changes in mechanical properties in pure collagen gels. First, we note that for AS collagen with CS, G′ displays a maximum at the intermediate CS concentration of 5.0 mg/ml even though mesh size increases monotonically as CS increases from 0 to 20.0 mg/ml. This is similar to the behavior seen in AS collagen gels at a given concentration gelled at different temperatures, where mesh size increases monotonically as a function of decreasing gelation temperature but stiffness first increases and then decreases with lower gelation temperature. This behavior is attributed to the fact that network storage modulus depends on not only network mesh size but also the stiffness of the struts that comprise the network [8].

Qualitatively, the fiber bundles present in the AS collagen/CS gels with the highest CS concentration look similar to those present in pure AS gels constructed at 32°C and do not exhibit as much bundling as those formed at lower temperatures [8]. We compare the correlation of mesh size and storage modulus for gels of 1.0 mg/ml AS collagen formed as a function of temperature and those formed at 37°C with added CS (Fig. 5a). Fig. 5a demonstrates that while the changes of mesh size and storage modulus are qualitatively similar for AS gels formed as a function of decreasing temperature and those formed in the presence of increasing CS in terms of maximum storage modulus occurring at intermediate mesh size, quantitatively the behavior of these two types of gels is quite different. The variation in G' is much stronger as a function of mesh size with the addition of CS than for pure 1.0 mg/ml AS collagen gelled at different temperatures. This suggests that CS itself affects the mechanical properties of the fibrils or interfibrillar interactions beyond effects from the collagen bundling it induces. One way in which the CS may alter the mechanical properties of the network is through stiffening or weakening the fibrils or fibers once incorporated into the collagen fibrils. Additionally, the presence of CS may alter the amount of collagen incorporated into the fibrils, thus altering mechanical properties [33, 35]. As such, we compare the CS mechanical properties and network structural properties to pure AS gels over a range of concentrations. In previous work, we found that AS collagen gel elastic moduli could be described in terms of network structural parameters from 0.5 – 4.0 mg/ml and gelation temperatures from 22°C – 37°C via $G' \sim \xi^{-22/5} d^{28/5}$ consistent with predictions of a semi-flexible polymer theory [42]. Here, ξ is mesh size and d is the average diameter of the bundled fiber structure when bundles are present and the individual fibril diameter when no bundling is observed. Assuming that AS collagen/CS gel moduli also display this behavior allows estimation of the fibril diameter present in the AS collagen/CS gels, as shown in Figure 5b. The range of predicted fibril diameters is physically reasonable, with a prediction of 52 nm at 0 mg/ml CS (as compared to 56 nm measured for such gels using SEM previously [8]) to a diameter of just over 90 nm, which correlates to bundles of ~ 4 fibrils. We conclude that AS collagen/CS gels exhibit changes in structure and network structural parameters that are consistent with those seen for pure AS collagen gels (Fig. 5b) in that both are well described by a semi-flexible polymer theory [42].

3.4 Influence of HA and CS on the Spheroid Invasion in Collagen Matrices

As described above, incorporation of GAGs into collagen matrices can induce changes in structural, mechanical, and biochemical properties of the matrices, each of which can affect cell behavior. In order to elucidate the biochemical effects of HA and CS on glioma

invasion, we study the growth of glioma spheroids in pure 1.0 mg/ml AS and PT collagen gels as well as AS and PT collagen gels with 10.0 mg/ml CS or HA.

Glioma MTSs are implanted in collagen and collagen/GAG gels. Two hours after implantation, collagen fibers surrounding the MTS are imaged (Fig. 6, bottom). The structure of the collagen networks surrounding the spheroids is similar to those found in cell-free gels (Fig. 1). MTS spheroid growth and invasion are monitored over time for 72 hours. Invasive distance is calculated as the distance between the dense spheroid body and the average extent of invasive cells. Invasive character and distance in pure AS and PT collagen gels are similar, with significant invasion evident (Fig. 6a,b; Fig 7). Cells demonstrate the migratory phenotype that has been seen previously for glioma cells in collagen gels, in which the cells extend along collagen fibers, exert traction on those fibers, release from the back end, and move forward [2]. In both AS and PT collagen gels, cells align collagen fibers into an astral pattern within several hours after spheroid placement in the collagen gel and then invade along these aligned fibers. While invasion in AS and PT gels is similar, invasion appears somewhat more aggressive in the AS gels, both in terms of invasive distance and invasive density, as the invasive front appears consistently denser in the AS gels than the PT gels of the same concentration.

Invasion in collagen/CS gels is inhibited relative to in pure AS and PT collagen gels, with fewer cells emerging from the dense spheroid body and their speed reduced relative to that in the pure collagen gels. While invasive distance is reduced in both AS/CS and PT/CS gels, the invasion in AS/CS matrices is more significantly hindered relative to in its pure counterpart than is the invasion in PT/CS gels (Fig. 7). Indeed, despite qualitative differences between invasion in collagen and collagen/CS matrices, it is only differences in invasive distance between C6 spheroids in AS and AS/CS gels that are statistically significant.

Invasion in collagen/HA gels is qualitatively similar to that in pure collagen gels, though the cells adopt a somewhat less elongated morphology and the density of invading cells is somewhat higher than that in pure collagen gels. In PT collagen, the presence of HA somewhat reduces invasive distance relative to invasion in pure PT collagen, especially at 24 and 48 hours. In AS collagen, this invasion inhibition is also seen at early times, but by 72 hours after implantation, invasive distance is more substantial in AS/HA gels than in pure AS gels.

4. Discussion

Single-component collagen matrices have been widely used as 3D ECM mimics to study *in vitro* cell migration including glioma cell invasion [2, 14–16, 20, 21]. However, gliomas in brain tissue encounter a variety of ECM components other than collagen as they invade either through brain parenchyma or along blood vessels, one of the preferential routes of invasion. GAGs including CS and HA are major components in brain ECM and are also found at elevated levels around brain tumors [43]. In order to better model the ECM of brain tissue for glioma invasion studies, CS and HA are incorporated into collagen gels.

The structural and mechanical properties of collagen/CS or HA composite gels are studied over a range of concentrations that encompass physiological concentration of CS and HA in a variety of tissues including brain. We find that AS collagen networks are more significantly affected structurally and mechanically by the presence of CS than PT collagen networks. CS increases fiber thickness and mesh size substantially in AS collagen-based matrices. The bundling of fibrils into fibers that occurs at high CS concentrations in AS collagen but not in PT collagen is reminiscent of the behavior of these two types of collagen

when gelled at temperatures of 32°C and below, where AS collagen fibrils bundle but PT collagen fibrils do not [8, 41]. This suggests that fibril bundling is strongly inhibited by the absence of telopeptides even when gelation is performed at conditions that induce significant bundling in AS collagen. Our observations on gel structure in the presence of CS A are generally consistent with the structural changes found when small amounts of CS C are added to AS collagen I networks [33, 35]. Our results differ somewhat from those of Douglas et al., where both CS A and CS C were found to decrease fibril diameter [32]. However, some fibril bundling in the presence of CS is evident in that study, and another study also suggests that high CS concentration can induce fibril bundling [28].

The storage modulus of PT collagen decreases slightly with CS concentration consistent with slightly increased mesh size in those gels. However, storage modulus of AS collagen shows a maximum at intermediate CS concentration, in a manner consistent with the increase of mesh size and fiber thickness seen in these gels as well as in pure AS collagen (Fig. 5). This confirms that storage modulus is a function of both fiber dimension and organization [8] and that collagen/CS matrix mechanical properties are dominated by collagen viscoelasticity.

As with the addition of CS, AS collagen is more significantly affected structurally than is PT collagen upon addition of HA. More numerous and thinner collagen fibrils are apparent with increasing HA concentration in AS collagen and to a lesser extent in PT collagen. We note that while HA itself forms a meshwork, there is no evidence it forms structures that can be visualized with CRM; instead, as suggested previously, it is likely HA co-localizes with collagen fibrils and/or remains homogeneously dispersed in between fibrils [31, 41, 44]. In our previous work, it was found that introducing 1.2 mg/ml HA during PT collagen assembly slightly decreased fibril width and slightly enhanced storage modulus relative to pure PT collagen [41]. Here, at higher HA concentrations in PT collagen, we find no stronger effect on gel structure but a very strong effect on gel strorage and viscous moduli, which are dominated by the HA mechanical response as reflected in the loss tangent. In AS collagen, the mechanical property changes induced by HA are similar to those seen in PT collagen, but the structural changes are more obvious, with more numerous fibrils present, resulting in decreased mesh size. Taking together the effects of CS and HA on AS and PT collagen, it is found that AS collagen is more substantially affected both structurally and mechanically by the presence of GAG molecules. This suggests that the non-helical ends of collagen may be crucial in controlling *in vivo* collagen self-assembly as it occurs in the presence of other ECM molecules.

We monitor the growth and invasion of spheroids in collagen gels with 10 mg/ml CS or HA because PT collagen gel structure is largely unaffected by the presence of the GAGs at that concentration while AS collagen gel structure is substantially affected. Additionally, PT and AS collagen storage moduli are not strongly affected by the presence of CS at this concentration. Indeed, differences of stiffness much larger than that between pure collagen and collagen gels with 10 mg/ml CS were shown not to affect spheroid invasion so long as mesh size was held constant in a previous study in pure AS collagen gels [10]. For the addition of 10 mg/ml HA, both PT and AS collagen gel moduli are affected; however, the effect is due in large measure to the presence of the highly viscous HA rather than induced changes to the collagen network.

Given that PT gel topology and collagen network based viscoelasticity do not change significantly with added CS or HA, we interpret changes in invasive success of spheroids in PT collagen/GAG environments to be dominated by the biochemical changes induced by the presence of the GAGs. However, because AS collagen/GAG environments demonstrate significant structural change in the presence of 10 mg/ml CS and HA, differences in growth

in these environments is expected to reflect both the biochemical presence of the GAGs as well as potential effects of the changes in the underlying network structure.

Our results indicate that C6 spheroids invade somewhat more aggressively in terms of invasive speed and cell density in AS collagen gels than in PT collagen gels. CS inhibits glioma invasion in both AS and PT collagen, though the difference is only statistically significant in the AS/CS gels. In PT collagen, any inhibition of invasion induced by the presence of CS is assumed to be related to CS biochemistry rather than changes to the structure and/or mechanical properties of collagen gels induced by CS, since structure and mechanical properties in PT collagen change very little with addition of CS. In AS collagen, there is a more substantial inhibition of invasion, potentially reflecting the biochemical effect of the CS plus the effect of a larger mesh size environment composed of fibril bundles, factors which may independently inhibit the migration of glioma cells through limiting cell ability to exert traction on and remodel the surrounding collagen structures [10]. The mechanism by which the biochemistry of CS may reduce invasion is not immediately clear. It has been found that CS A can increase adhesion of osteoblasts to collagen fibrils [32]. While such interactions do not necessarily suggest decreased invasion, if the presence of CS enhances cell-collagen adhesion substantially, this may prevent cell release from the collagen fibrils, thus preventing invasion deep into the collagen matrix [45, 46].

While CS inhibits glioma invasion, HA appears to have limited effect on invasion in PT and AS collagen gels, with some evidence that HA encourages growth at long times in AS collagen gels. It has been shown previously that HA can facilitate glioma invasion [23, 47, 48] though one study shows HA oligomers may limit the malignant behavior of gliomas [49]. *In vivo*, it has been suggested that HA can facilitate invasion through absorbing water and enlarging the pericellular space, providing space through which the cells could migrate. *In vitro* in 1.0 mg/ml gels, which display a mesh size amenable to cell migration, this factor is not expected to come into play. Indeed, we see a decrease in mesh size as a function of increasing HA concentration in both PT and AS collagen based matrices. The fact that HA appears to slow invasion at early times in both PT and AS based matrices may suggest that the increased viscoelasticity of the system at early times inhibits invasion. Late invasion, however, accelerates in both types of gels, with a more noticeable increase occurring in AS collagen-based gels. These effects may be due to a combination of HA's effects on the biochemistry of the environment and a contribution from the increased number and decreased width of fibrils seen in the presence of HA, as in this mesh size range increased fibril number enhances invasive density and speed by allowing for more cells to generate traction on and move along particular fibrillar structures. This is consistent with the higher density of invasive cells seen in the HA containing gels relative to either the pure collagen gels or the CS containing gels.

5. Conclusion

Composite matrices containing collagen and either CS or HA were constructed to enhance similarity between the *in vitro* environment and brain tissue ECM. The structure and mechanical properties of collagen/CS and collagen/HA gels were studied via CRM and rheology. It was found that AS collagen network structure is affected by both CS and HA, while PT collagen network structure is largely unaffected. Moreover, the mechanical properties of AS collagen-based gels are more substantially affected by the presence of CS than are PT gels, suggesting the source of the change is the alteration in collagen network structure. Indeed, the relationship between microstructure and storage modulus in AS/CS gels demonstrates that, in cases in which the secondary component does not itself have a complex viscoelastic behavior, gel storage modulus is determined by both fiber diameter and

network mesh size. The effects of CS and HA on glioma invasion were then studied in collagen/GAG matrices with structure both similar to (PT collagen-based gels) and different from (AS collagen-based gels) those of pure collagen matrices. From these studies, it appears that cell invasion in AS collagen-based gels is more substantially affected by the presence of secondary ECM components than in PT collagen-based gels. This highlights the fact that not only the biochemical effect but also any changes in collagen network structure induced by the secondary ECM component must be considered when evaluating cell behavior in composite environments.

Acknowledgments

This work was supported by a Beckman Young Investigator Award and a Camille Dreyfus Teacher Scholar Award to L.J.K., NSF 0754919 (L.J.F.) and NSF DGE 0801530 (C.S. and M.E.W.), and NIH RC1GM091804.

References

1. Alberts, B.; Johnson, A.; Lewis, J.; Raff, M.; Roberts, K.; P, W. Molecular Biology of the Cell. New York: Garland Science; 2002.
2. Kaufman LJ, Brangwynne CP, Kasza KE, Filippidi E, Gordon VD, Deisboeck TS, et al. Glioma expansion in collagen I matrices: Analyzing collagen concentration-dependent growth and motility patterns. Biophys J. 2005; 89(1):635–650. [PubMed: 15849239]
3. Wolf K, Mazo I, Leung H, Engelke K, von Andrian UH, Deryugina EI, et al. Compensation mechanism in tumor cell migration: Mesenchymal-amoeboid transition after blocking of pericellular proteolysis. J Cell Biol. 2003; 160(2):267–277. [PubMed: 12527751]
4. Cukierman E, Pankov R, Yamada KM. Cell interactions with three-dimensional matrices. Curr Opin Cell Biol. 2002; 14(5):633–639. [PubMed: 12231360]
5. Wood GC, Keech MK. The formation of fibrils from collagen solutions. 1. The effect of experimental conditions: Kinetic and electron-microscope studies. Biochem J. 1960:75588–75598.
6. Raub CB, Unruh J, Suresh V, Krasieva T, Lindmo T, Gratton E, et al. Image correlation spectroscopy of multiphoton images correlates with collagen mechanical properties. Biophys J. 2008; 94(6):2361–2373. [PubMed: 18065452]
7. Raub CB, Suresh V, Krasieva T, Lyubovitsky J, Mih JD, Putnam AJ, et al. Noninvasive assessment of collagen gel microstructure and mechanics using multiphoton microscopy. Biophys J. 2007; 92(6):2212–2222. [PubMed: 17172303]
8. Yang, Y-l; Leone, LM.; Kaufman, LJ. Elastic moduli of collagen gels can be predicted from two dimensional confocal microscopy. Biophys J. 2009; 97(7):2051–2060. [PubMed: 19804737]
9. Zaman MH, Trapani LM, Siemeski A, MacKellar D, Gong HY, Kamm RD, et al. Migration of tumor cells in 3D matrices is governed by matrix stiffness along with cell-matrix adhesion and proteolysis. Proc Natl Acad Sci U S A. 2006; 103(29):10889–10894. [PubMed: 16832052]
10. Yang, Y-l; Motte, S.; Kaufman, LJ. Pore size variable type I collagen gels and their interactions with glioma cells. Biomaterials. 2010; 31(21):5678–5688. [PubMed: 20430434]
11. Bailey JL, Critser PJ, Whittington C, Kuske JL, Yoder MC, Voytik-Harbin SL. Collagen oligomers modulate physical and biological properties of three-dimensional self-assembled matrices. Biopolymers. 95(2):77–93. [PubMed: 20740490]
12. Pathak A, Kumar S. Biophysical regulation of tumor cell invasion: Moving beyond matrix stiffness. Integr Biol. 3(4):267–278.
13. Pizzo AM, Kokini K, Vaughn LC, Waisner BZ, Voytik-Harbin SL. Extracellular matrix (ecm) microstructural composition regulates local cell-ECM biomechanics and fundamental fibroblast behavior: A multidimensional perspective. J Appl Physiol. 2005; 98(5):1909–1921. [PubMed: 15618318]
14. Gordon VD, Valentine MT, Gardel ML, Andor-Ardo D, Dennison S, Bogdanov AA, et al. Measuring the mechanical stress induced by an expanding multicellular tumor system: A case study. Exp Cell Res. 2003; 289(1):58–66. [PubMed: 12941604]

15. Hegedus B, Marga F, Jakab K, Sharpe-Timms KL, Forgacs G. The interplay of cell-cell and cell-matrix interactions in the invasive properties of brain tumors. Biophys J. 2006; 91(7):2708–2716. [PubMed: 16829558]
16. Kim HD, Guo TW, Wu AP, Wells A, Gertler FB, Lauffenburger DA. Epidermal growth factor-induced enhancement of glioblastoma cell migration in 3d arises from an intrinsic increase in speed but an extrinsic matrix- and proteolysis-dependent increase in persistence. Mol Biol Cell. 2008; 19(10):4249–4259. [PubMed: 18632979]
17. Stein AM, Demuth T, Mobley D, Berens M, Sander LM. A mathematical model of glioblastoma tumor spheroid invasion in a three-dimensional in vitro experiment. Biophys J. 2007; 92(1):356–365. [PubMed: 17040992]
18. Tamaki M, McDonald W, Amberger VR, Moore E, DelMaestro RF. Implantation of C6 astrocytoma spheroid into collagen type I gels: Invasive, proliferative, and enzymatic characterizations. J Neurosurg. 1997; 87(4):602–609. [PubMed: 9322849]
19. Werbowetski T, Bjerkvig R, Del Maestro RF. Evidence for a secreted chemorepellent that directs glioma cell invasion. J Neurobiol. 2004; 60(1):71–88. [PubMed: 15188274]
20. Del Maestro R, Shivers R, McDonald W, Del Maestro A. Dynamics of c-6 astrocytoma invasion into three-dimensional collagen gels. J Neurooncol. 2001; 53(2):87–98. [PubMed: 11716073]
21. An Z, Gluck CB, Choy ML, Kaufman LJ. Suberoylanilide hydroxamic acid limits migration and invasion of glioma cells in vitro. Cancer Lett. 2010:292215–292227.
22. Giese A, Westphal M. Glioma invasion in the central nervous system. Neurosurgery. 1996; 39(2): 235–250. [PubMed: 8832660]
23. Toole BP. Hyaluronan: From extracellular glue to pericellular cue. Nature Reviews Cancer. 2004; 4(7):528–539.
24. Koochekpour S, Pilkington GJ, Merzak A. Hyaluronic-acid CD44 interaction induces cell detachment and stimulates migration and invasion of human glioma-cells in-vitro. Int J Cancer. 1995; 63(3):450–454. [PubMed: 7591247]
25. Giese A, Bjerkvig R, Berens ME, Westphal M. Cost of migration: Invasion of malignant gliomas and implications for treatment. J Clin Oncol. 2003; 21(8):1624–1636. [PubMed: 12697889]
26. Viapiano MS, Matthews RT. From barriers to bridges: Chondroitin sulfate proteoglycans in neuropathology. Trends Mol Med. 2006; 12(10):488–496. [PubMed: 16962376]
27. Yamaguchi Y. Lecticans: Organizers of the brain extracellular matrix. Cell Mol Life Sci. 2000; 57(2):276–289. [PubMed: 10766023]
28. Turley EA, Erickson CA, Tucker RP. The retention and ultrastructural appearances of various extracellular matrix molecules incorporated into three-dimensional hydrated collagen lattices. Dev Biol. 1985; 109(2):347–369. [PubMed: 2581830]
29. Scott JE. Proteoglycan-fibrillar collagen interactions. Biochem J. 1988; 252(2):313–323. [PubMed: 3046606]
30. Tsai SW, Liu RL, Hsu FY, Chen CC. A study of the influence of polysaccharides on collagen self-assembly: Nanostructure and kinetics. Biopolymers. 2006; 83(4):381–388. [PubMed: 16826588]
31. Salchert K, Streller U, Pompe T, Herold N, Grimmer M, Werner C. In vitro reconstitution of fibrillar collagen type I assemblies at reactive polymer surfaces. Biomacromolecules. 2004; 5(4): 1340–1350. [PubMed: 15244449]
32. Douglas T, Heinemann S, Mietrach C, Hempel U, Bierbaum S, Scharnweber D, et al. Interactions of collagen types I and II with chondroitin sulfates A and C and their effect on osteoblast adhesion. Biomacromolecules. 2007; 8(4):1085–1092. [PubMed: 17378603]
33. Stuart K, Panitch A. Influence of chondroitin sulfate on collagen gel structure and mechanical properties at physiologically relevant levels. Biopolymers. 2008; 89(10):841–851. [PubMed: 18488988]
34. Wood GC. The formation of fibrils from collagen solutions. 3. Effect of chondroitin sulphate and some other naturally occurring polyanions on the rate of formation. Biochem J. 1960; 75(3):605–612. [PubMed: 13845811]
35. Stuart K, Panitch A. Characterization of gels composed of blends of collagen I, collagen III, and chondroitin sulfate. Biomacromolecules. 2009; 10(1):25–31. [PubMed: 19053290]

36. Xin X, Borzacchiello A, Netti PA, Ambrosio L, Nicolais L. Hyaluronic-acid-based semi-interpenetrating materials. J Biomater Sci Polym Ed. 2004; 15(9):1223–1236. [PubMed: 15503636]
37. Hsu S, Jamieson AM, Blackwell J. Viscoelastic studies of extracellular-matrix interactions in a model native collagen gel system. Biorheology. 1994; 31(1):21–36. [PubMed: 8173042]
38. Kreger ST, Voytik-Harbin SL. Hyaluronan concentration within a 3D collagen matrix modulates matrix viscoelasticity, but not fibroblast response. Matrix Biol. 2009; 28(6):336–346. [PubMed: 19442729]
39. Zeugolis DI, Paul RG, Attenburrow G. Factors influencing the properties of reconstituted collagen fibers prior to self-assembly: Animal species and collagen extraction method. J Biomed Mater Res Part A. 2008; 86A(4):892–904.
40. Kreger ST, Bell BJ, Bailey J, Stites E, Kuske J, Waisner B, et al. Polymerization and matrix physical properties as important design considerations for soluble collagen formulations. Biopolymers. 93(8):690–707. [PubMed: 20235198]
41. Yang, Y-l; Kaufman, LJ. Rheology and confocal reflectance microscopy as probes of mechanical properties and structure during collagen and collagen/hyaluronan self-assembly. Biophys J. 2009; 96(4):1566–1585. [PubMed: 19217873]
42. Mackintosh FC, Kas J, Janmey PA. Elasticity of semiflexible biopolymer networks. Phys Rev Lett. 1995; 75(24):4425–4428. [PubMed: 10059905]
43. Bertolotto A, Magrassi ML, Orsi L, Sitia C, Schiffer D. Glycosaminoglycan changes in human gliomas - a biochemical-study. J Neurooncol. 1986; 4(1):43–48. [PubMed: 3746384]
44. Coleman PJ. Evidence for a role of hyaluronan in the spacing of fibrils within collagen bundles in rabbit synovium. Biochim Biophys Acta-Gen Subj. 2002; 1571(3):173–182.
45. Palecek SP, Loftus JC, Ginsberg MH, Lauffenburger DA, Horwitz AF. Integrin-ligand binding properties govern cell migration speed through cell-substratum adhesiveness. Nature. 1997; 385(6616):537–540. [PubMed: 9020360]
46. Gaudet C, Marganski WA, Kim S, Brown CT, Gunderia V, Dembo M, et al. Influence of type i collagen surface density on fibroblast spreading, motility, and contractility. Biophys J. 2003; 85(5):3329–3335. [PubMed: 14581234]
47. Rutka JT, Apodaca G, Stern R, Rosenblum M. The extracellular-matrix of the central and peripheral nervous systems - structure and function. J Neurosurg. 1988; 69(2):155–170. [PubMed: 3292716]
48. Giese A, Loo MA, Rief MD, Tran N, Berens ME. Substrates for astrocytoma invasion. Neurosurgery. 1995; 37(2):294–301. [PubMed: 7477782]
49. Ward JA, Huang L, Guo HM, Ghatak S, Toole BP. Perturbation of hyaluronan interactions inhibits malignant properties of glioma cells. Am J Pathol. 2003; 162(5):1403–1409. [PubMed: 12707023]

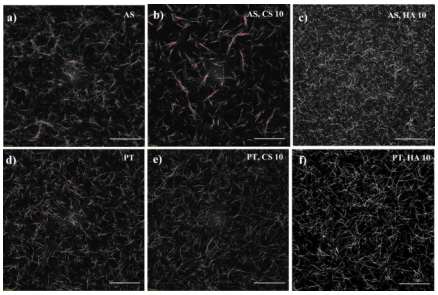

Figure 1.

CRM images of 1.0 mg/ml (a) AS collagen, (b) AS collagen with 10 mg/ml CS, (c) AS collagen with 10 mg/ml HA, (d) PT collagen, (e) PT collagen with 10 mg/ml CS, and (f) PT collagen with 10 mg/ml HA. Scale bars are 50 μm.

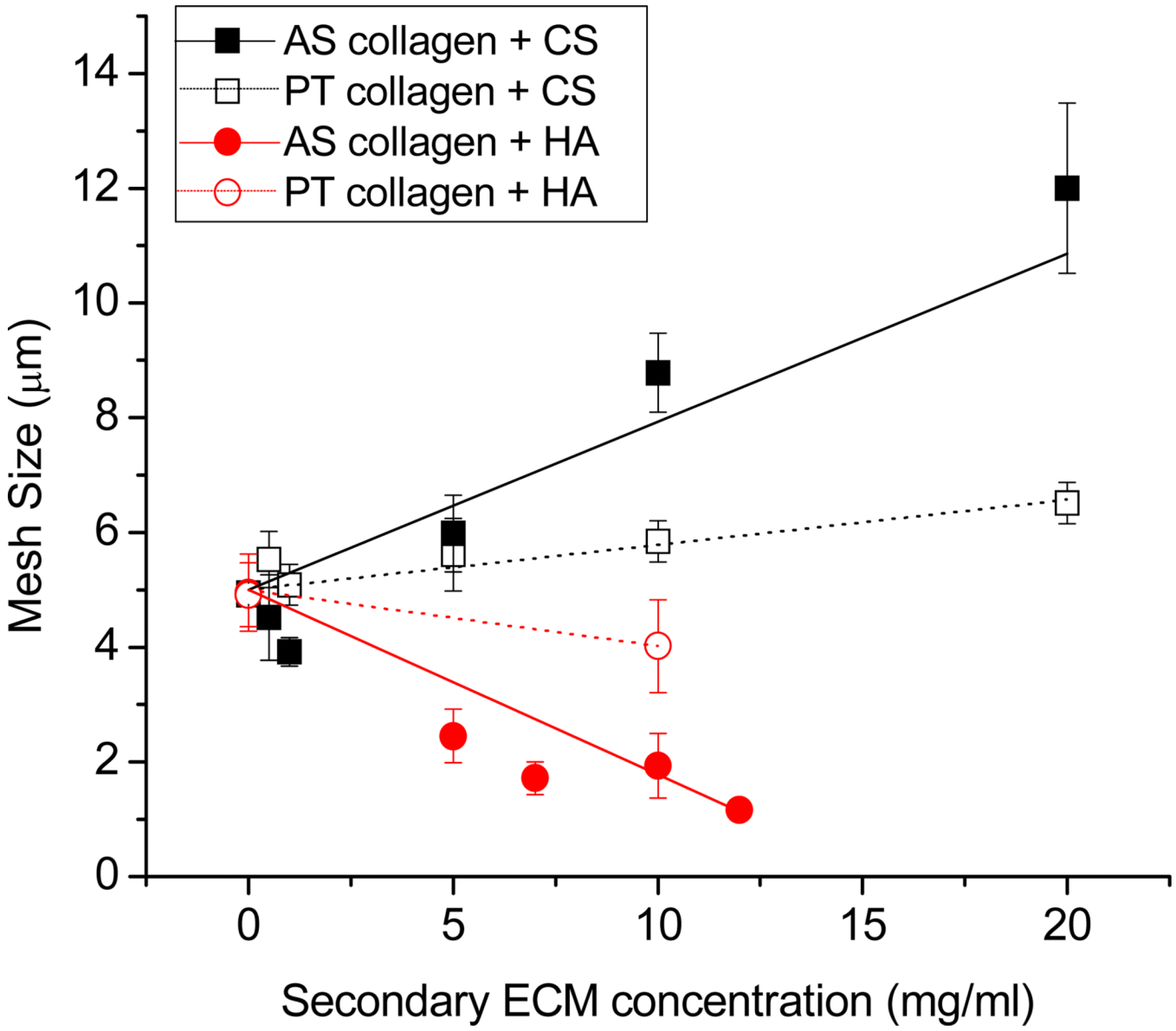

Figure 2.
Mesh size as a function of CS and HA concentration for AS and PT collagen. Best-fit lines to the data are shown. AS collagen with CS (black solid squares and line), PT collagen with CS (black open squares and dashed line), AS collagen with HA (red solid circles and line), and PT collagen with HA (red open circles and dashed line). Each point represents the average of nine images (collected from three gels) and error bars represent standard deviations.

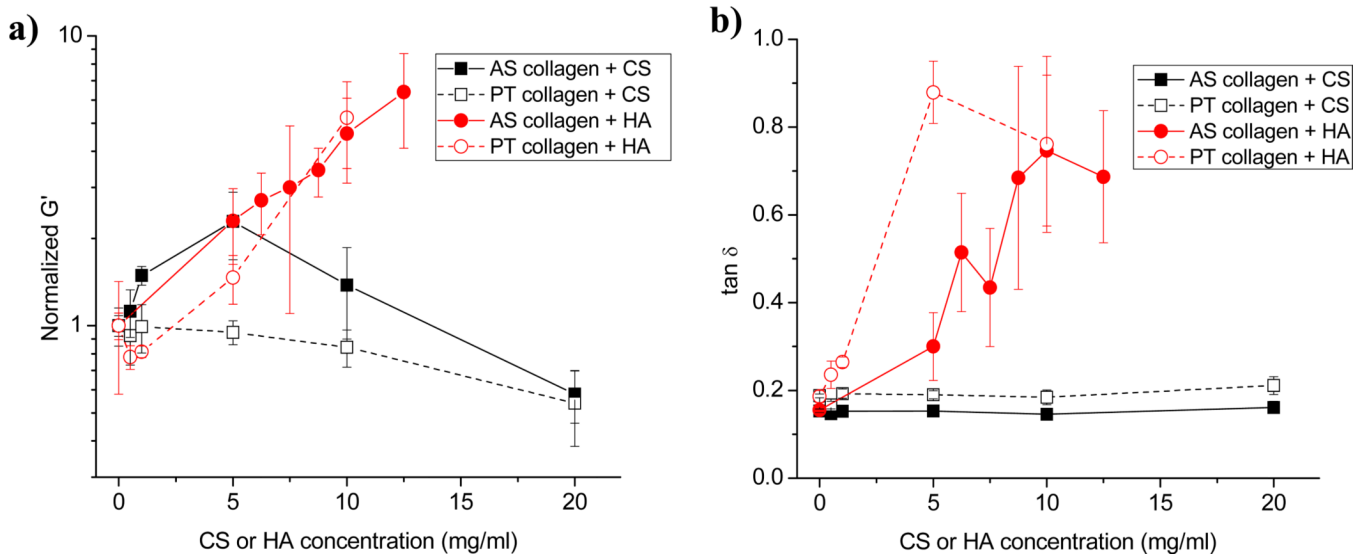

Figure 3.

(a) Storage moduli of AS collagen with CS (black solid squares and line), PT collagen with CS (black open squares and dashed line), AS collagen with HA (red solid circles and line), and PT collagen with HA (red open circles and dashed line). Moduli are normalized to pure AS or PT collagen at 1.0 mg/ml. (b) Loss tangent (tan δ = G”/G’) for AS and PT collagen with CS and HA. Symbols are the same as in (a). In all cases, each point represents the average of 3 or 4 measurements and error bars represent standard deviations.

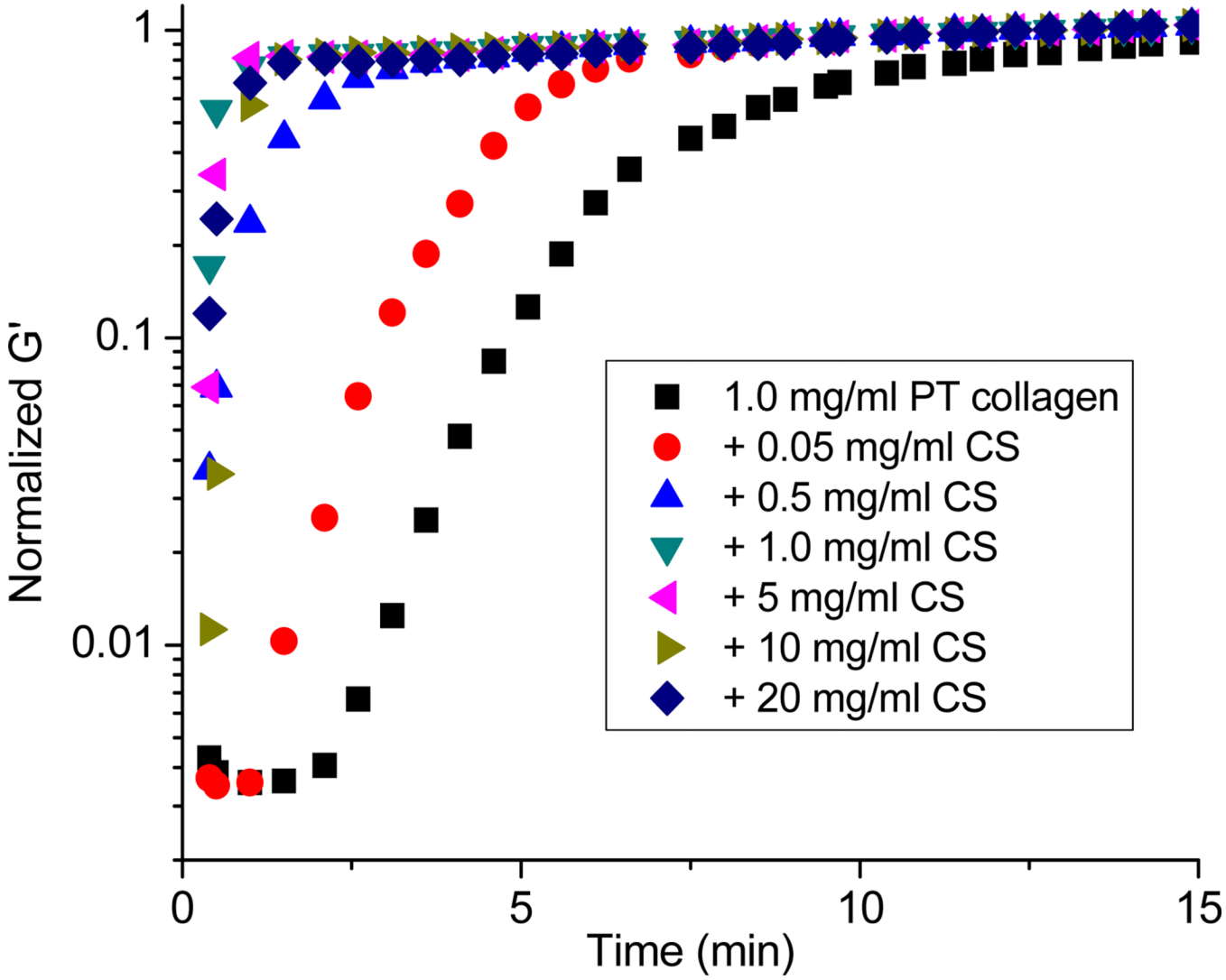

Figure 4.
Normalized oscillatory time sweep of 1.0 mg/ml PT collagen without (black square) or with CS (red circle, 0.05 mg/ml; blue upright triangle, 0.5 mg/ml; green downright triangle, 1.0 mg/ml; pink left triangle, 5 mg/ml; olive right triangle, 10 mg/ml; blue diamond, 20 mg/ml). All traces represent three averaged time sweeps and all are normalized to the modulus measured at 30 minutes.

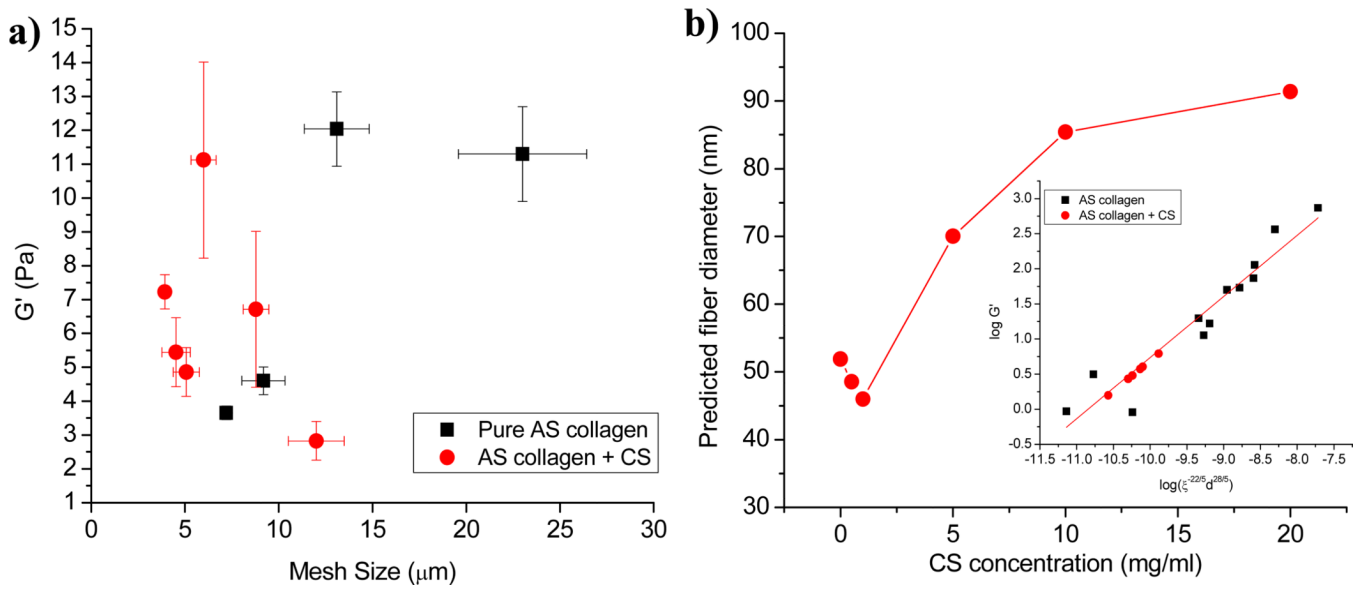

Figure 5.

(a) Plateau storage modulus vs. mesh size for 1.0 mg/ml AS collagen gels with 0, 0.5, 1.0, 5.0, 10.0, and 20.0 mg/ml CS gelled at 37°C (red circles) and for 1.0 mg/ml AS collagen gelled at 37°C, 32°C, 27°C, or 22°C (black squares). (b) Predicted fiber diameter of AS collagen as a function of CS concentration using the relationship between storage modulus, mesh size, and fibrillar diameter determined to fit behavior of pure AS collagen over a range of concentrations and gelation temperatures: $\log(G') = 0.871(\log(\xi^{-22/5}d^{28/5})) + 9.4$, with ξ mesh size and d, fiber diameter [8] with d allowed to vary. Inset shows fit of AS collagen/CS data to the equation for the best fit d values. Black squares are data from Reference [8] and red circles are data from AS collagen/CS gels.

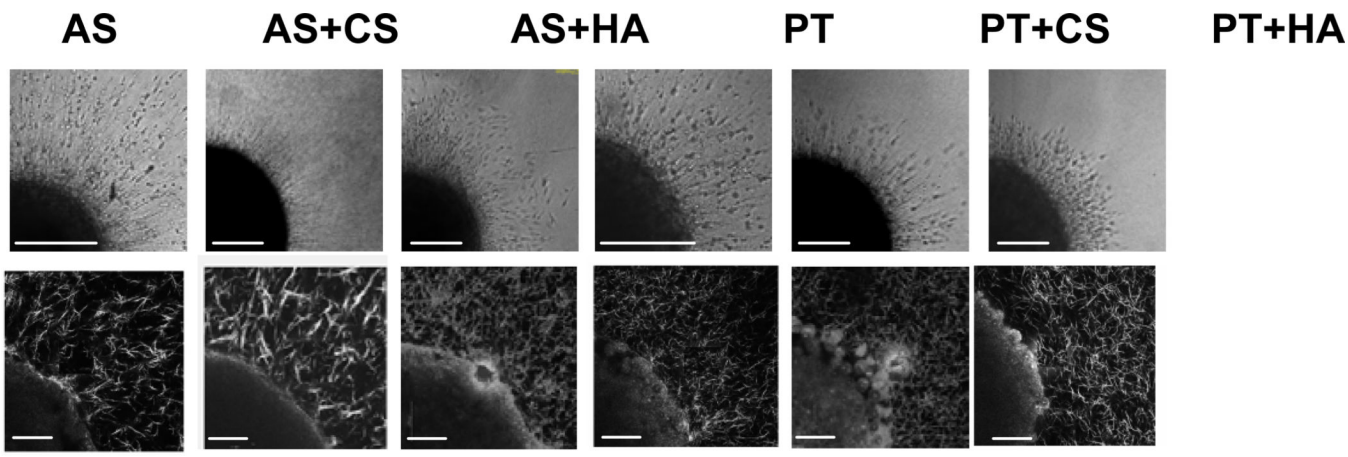

Figure 6.

C6 spheroid invasion in, left to right, 1.0 mg/ml AS collagen, 1.0 mg/ml AS collagen with 10 mg/ml CS, 1.0 mg/ml AS collagen with 10 mg/ml HA, 1.0 mg/ml PT collagen, 1.0 mg/ml PT collagen with 10 mg/ml CS, and 1.0 mg/ml PT collagen with 10 mg/ml HA. (top) Representative transmittance images of invading spheroid 24 hours after implantation. One quarter of the spheroid and invading cells is shown. Scale bars are 200 μm. (bottom) Representative CRM images of one quarter of the spheroid and surrounding collagen fibers 2 hours after implantation. Scale bars are 50 μm. Spheroids pictured in CRM images are not necessarily the same spheroids as those pictured in the transmittance images.

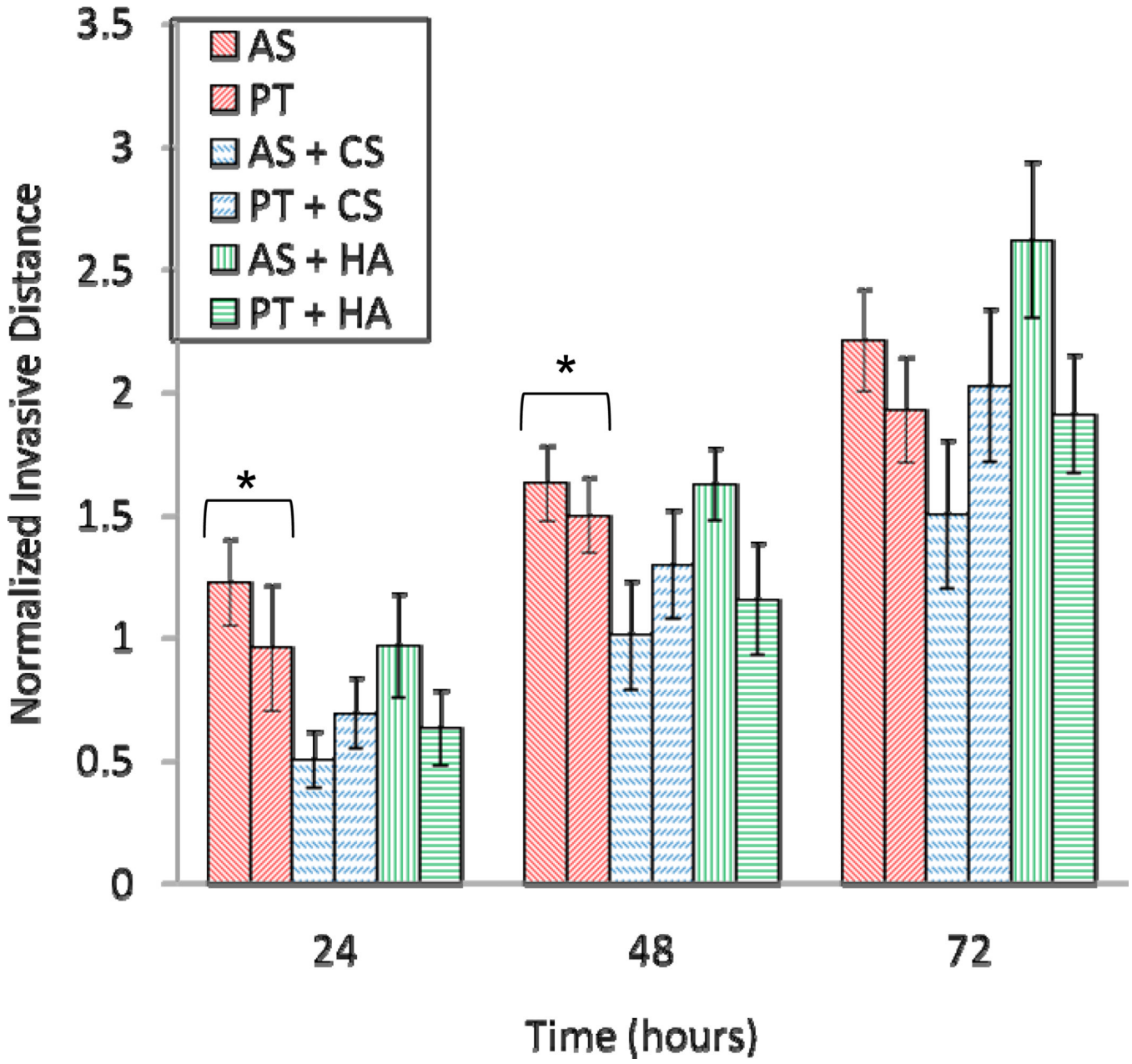

Figure 7.

C6 spheroid invasive distance normalized by initial spheroid radius as a function of time for spheroids in AS collagen (red, right diagonal stripes), PT collagen (red, left diagonal stripes), AS collagen with 10 mg/ml CS (blue, right dashed diagonal stripes), PT collagen with 10 mg/ml CS (blue, left dashed diagonal stripes), AS collagen with 10 mg/ml HA (green, vertical stripes), PT collagen with 10 mg/ml HA (green, horizontal stripes). Six spheroids were measured in each type of gel and error bars represent standard errors. Asterisks indicate statistically significant results as assessed by two-tailed unpaired t-tests, with p values < 0.05. t-tests were performed at 24, 48, and 72 hours for AS vs. AS-CS, AS vs. AS-HA, PT vs. PT-CS, PT vs. PT-HA, AS vs. PT, AS-CS vs. PT-CS, and AS-HA vs. PT-HA.